Piperidine Glycosides Targeting the Ribosomal Decoding Site

Klaus B. Simonsen,*[a] Benjamin K. Ayida,[a] Dionisios Vourloumis,[a] Geoffrey C. Winters,[a] Masayuki Takahashi,[a] Sarah Shandrick,[b] Qiang Zhao,[b] and Thomas Hermann*[b]

KEYWORDS:

aminoglycosides · antibiotics · drug design · medicinal chemistry · RNA recognition

As has been outlined in the accompanying report,[1] synthetic aminoglycoside mimetics constitute lead compounds for the development of novel antibiotics that might achieve antibacterial potency comparable to the natural aminoglycosides without being compromised by bacterial resistance mechanisms specific to the chemical constitution of these natural compounds. Three-dimensional structures of the bacterial decoding-site RNA complexed with aminoglycosides[2, 3] have guided our efforts for rational, structure-based design of readily accessible aminoglycoside mimetics (Figure 1).

In this report, we outline a novel approach to linking the 6′-aminoglucosamine moiety, conserved among many potent natural aminoglycosides, to conformationally restricted 3-(aminomethyl)piperidine scaffolds that mimic the unique spatial arrangement of functional groups in 2-deoxystreptamine (2-DOS) required for the recognition of the decoding-site RNA target (Figure 1 c – e). The exocyclic bis-equatorial 1,3-diamine motif of 2-DOS is incorporated into the cyclic piperidine scaffold, which was designed by molecular modeling[4] based on the crystal structure of paromomycin bound to the bacterial decoding site (Figure 1).[2] Three different substitution patterns have been used to generate eight piperidine derivatives of glucosamine (see Table 1), among them the representative hydroxymethyl compound **1** (Figure 1 c). The 5-hydroxymethyl substituent in the piperidine glycoside **1** was designed to mimic the 4-hydroxy group of paromamine (Figure 1 d), which forms a key interaction with a tightly bound water molecule at the deep-groove edge of the U1406◦U1495 base pair in the decoding-site target (Figure 1 e).[3] Several other piperidine glycosides were synthesized to explore alternative substitution patterns of the 3-(aminomethyl)piperidine scaffold (see Table 1).

[a] *Dr. K. B. Simonsen, Dr. D. Vourloumis, Dr. B. K. Ayida, G. C. Winters, M. Takahashi*
Department of Medicinal Chemistry
Anadys Pharmaceuticals, Inc.
9050 Camino Santa Fe, San Diego, CA 92121 (USA)
E-mail: ksimonsen@anadyspharma.com

[b] *Dr. T. Hermann, S. Shandrick, Dr. Q. Zhao*
Departments of RNA Biochemistry and Structural Chemistry
Anadys Pharmaceuticals, Inc.
9050 Camino Santa Fe, San Diego, CA 92121 (USA)
Fax: (+1) 858-527-1539
E-mail: thermann@anadyspharma.com

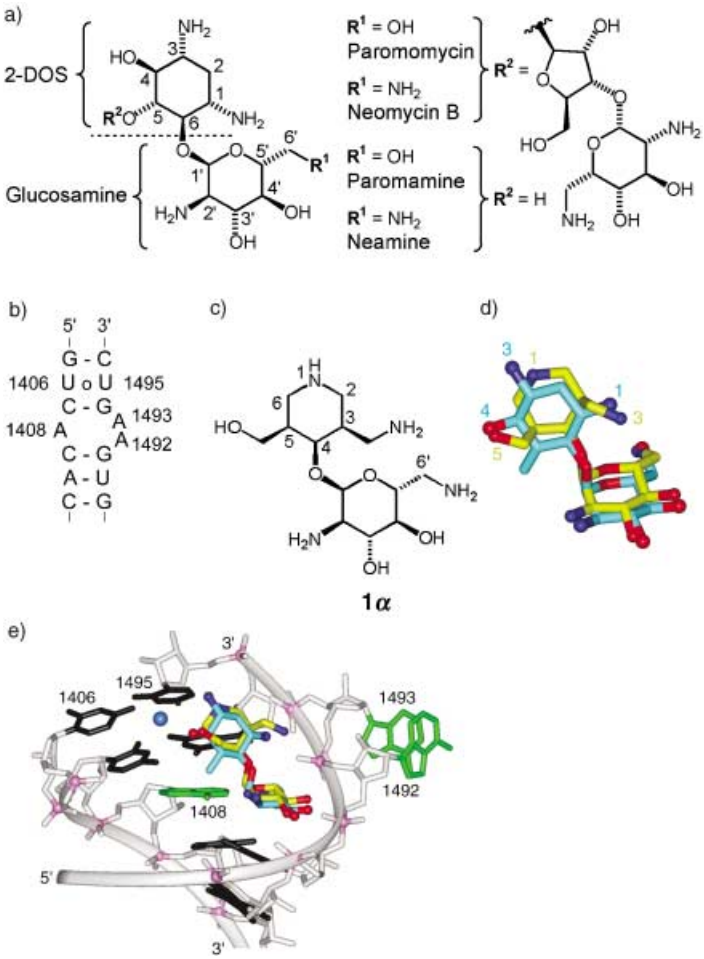

*Figure 1. a) Potent natural aminoglycoside antibiotics such as paromomycin and neomycin B are derived from paromamine and neamine, which share the 2-deoxystreptamine (2-DOS) and glucosamine cores, both of which are involved in RNA molecular recognition. b) Secondary structure of the bacterial decoding-site RNA, the target of natural aminoglycosides. c) Representative designed piperidine glycoside ligand **1** for the decoding-site RNA, derived by coupling 6′-aminoglucosamine with a 3-(aminomethyl)piperidine moiety acting as a 2-DOS mimetic. d) Three-dimensional model of the designed piperidine glycoside (yellow) superimposed on paromamine (blue), showing their conformational similarity. For clarity, the superimposed molecules have been slightly shifted along the y-axis. Numbering schemes for paromamine and the piperidine glycoside are shown in the corresponding colors. The 5-hydroxymethyl substituent in the piperidine derivative coincides with the 4-hydroxy group of paromamine, and the exocyclic 3-amino functionality of paromamine is replaced by the intracyclic secondary amine group in the piperidine ring. e) Model of the piperidine glycoside **1** (yellow) docked in the three-dimensional structure[2] of the bacterial decoding-site RNA in complex with paromomycin (blue; only paromamine core shown). RNA bases, dark grey; sugar – phosphate backbone, light grey with phosphate groups in magenta. A water molecule participating in the non-Watson – Crick U1406◦U1495 base pair[3] and interacting with a 2-DOS hydroxy group is shown as a blue sphere. The flipped-out adenine residues 1492 and 1493, and the unpaired adenine 1408 are shown in green.*

The syntheses of the 3,5-disubstituted piperidines are outlined in Scheme 1. In order to circumvent the purification of isomeric mixtures, we decided to proceed with enantiopure compounds obtained by enzymatic transformations. Suitable enzymes for stereoselective conversions were selected from the variety of reliable transformations that have been developed over the last decade as powerful tools for the preparation of chiral building blocks.[5]

 © 2003 Wiley-VCH Verlag GmbH & Co. KGaA, Weinheim DOI: 10.1002/cbic.200300689

Table 1. *Structure – activity relationships for synthetic piperidine glycosides.*

Structure	Cpd n°	$B_{IVT}IC_{50}$ RNA IC_{50} MIC	$E_{IVT}IC_{50}$[a]
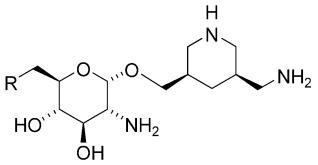	**7**, R = NH_2	260 n.d. > 64/ > 64	> 250
	8, R = OH	> 1000 n.d n.d.	> 250
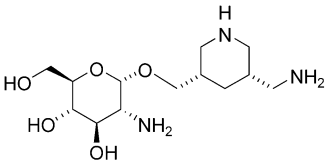	**11**	> 1000 n.d. n.d.	> 250
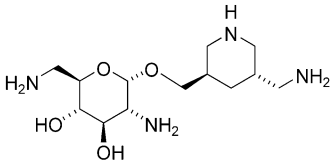	**15**	> 1000 n.d. n.d.	> 250
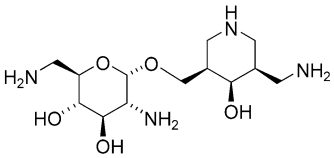	**27**	74 110 > 64/ > 64	> 250
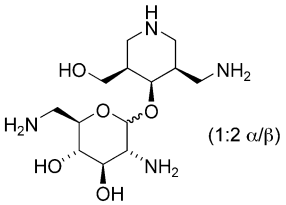 (1:2 α/β)	**1**	35 90 > 64/ > 64	> 250
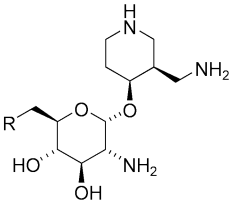	**20**, R = NH_2	> 1000 n.d. > 64/ > 64	> 250
	21, R = OH	> 1000 n.d. n.d.	> 250

[a] IC_{50}, concentration required for 50% inhibition. All IC_{50} values are in μM. B_{IVT}: IC_{50} value determined in a coupled bacterial in vitro transcription – translation assay with firefly luciferase reporter, as previously described;[9] IC_{50} values were calculated as the average of six replicate experiments for each compound (±10%). All compounds tested negative in counter-screens for luciferase and polymerase inhibition. E_{IVT}: IC_{50} value determined in a eukaryotic in vitro translation assay with firefly luciferase reporter; IC_{50} values were calculated as the average of three replicate experiments (±15%). RNA: IC_{50} value found in a fluorescence-based assay that measures RNA-binding affinity of compounds and their efficacy to flip-out the flexible adenine residues in a decoding site model oligonucleotide (±10%).[10] MIC: minimum inhibitory concentration [$\mu g\,mL^{-1}$], determined as the average of triplicate measurements in serial dilution, against *Escherichia coli* (first value) and *Staphylococcus aureus* (second value).

The central precursor for the diasteroselective synthesis of the piperidine glycosides **7**, **8**, and **11**, (3*R*,5*S*)-*N*-benzyloxycarbonyl-3-hydroxymethyl-5-acetoxymethylpiperidine (**3**), was prepared in six steps from pyridine-3,5-dicarboxylic acid (**2**) by using a lipase from *Pseudomonas fluorescens* in the resolution step, as reported by Lesma and coworkers (enantiomeric excess, *ee* > 98%; Scheme 1).[6] The synthetic route to the designed compounds **7** and **8** proceeded by cleavage of the Cbz protecting group by catalytic hydrogenation followed by reprotection of the transient amine with $(Boc)_2O$ in a single operation. Standard mesylation, followed by installation of the azido group and subsequent hydrolysis of the acetate group delivered the alcohol **4**, which was glycosylated with donor **5** or **6** in the presence of NIS and triflic acid to give the α-pseudodisaccharides as the only detectable anomers. A three-step deprotection protocol completed the synthesis of **7** and **8** (Scheme 1). Reversing the sequence used to introduce the amino functionality and the glycosylation step gave access to a compound with inverted stereochemistry on the piperidine scaffold. Thus, glycosylation of **9** under the conditions described above furnished **10** as the major anomer. Hydrolysis of the acetate group, followed by mesylation and subsequent azide introduction afforded product **11**, after removal of all protecting groups. The *trans*-substituted compound **12**, isolated during the synthesis of **3**, was converted into the mono-TBS-protected intermediate **13** in four steps, as depicted in Scheme 1. Mesylation followed by azide introduction and TBS removal yielded the alcohol **14**, which was glycosylated and deprotected as described above to produce the piperidine glycoside **15**.

The syntheses of 3,4-disubstituted piperidines, outlined in Scheme 2, commenced with reduction of the Boc-protected 4-keto-3-carboxylate **16** by treatment with bakers yeast.[7] The hydroxy group in **17** was protected with TBSCl, and the ester functionality reduced by treatment with $LiBH_4$ to produce **18**, which was converted to the corresponding azidomethyl compound as described previously (Scheme 1). Initial problems associated with instability of the Boc protection group in the glycosylation step were circumvented by replacing the Boc group with the trifluoroacetate group, under standard conditions. Finally, removal of the silicon group afforded alcohol **19**, which was glycosylated with **5** or **6**, followed by a three-step deprotection sequence to produce the piperidine glycosides **20** and **21**.

Our initial design dictated the attachment of a hydroxymethyl group onto the piperidine scaffold as an additional hydrogen-bond-donor moiety and a handle for potential functionalization. This process yielded the designed piperidine glycoside **1**. The syntheses of the 4-hydroxy (**27**) and 5-hydroxymethyl (**1**) analogues are summarized in Scheme 3. Dimethyl 4-hydroxypyridine-3,5-dicarboxylate (**22**) was converted into enantiomerically pure **23** in four steps by using a lipase from *Murcor javinicus* (lipase M) in the resolution step, as described by Bols et al.[8] As a precaution to prevent undesirable

 © 2003 Wiley-VCH Verlag GmbH & Co. KGaA, Weinheim

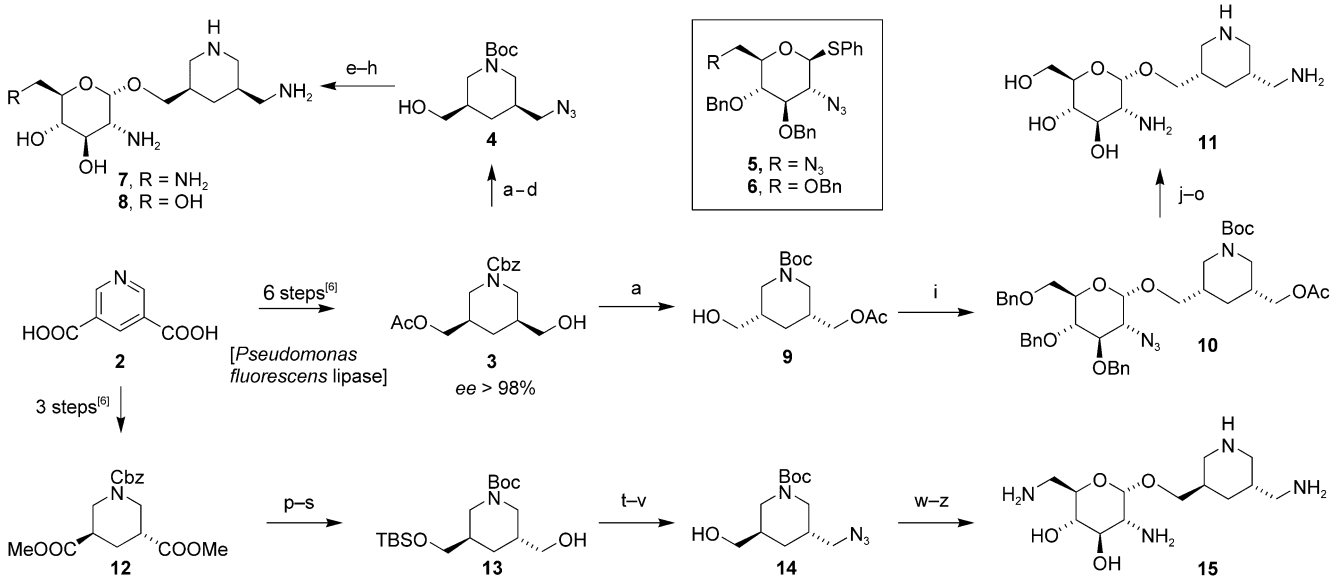

Scheme 1. Reagents and conditions: a) $(Boc)_2O$ (2.0 equiv), $Pd(OH)_2$ (0.05 equiv), H_2, EtOH (0.15 M), 20 h, 23 °C, 98%; b) MsCl (1.2 equiv), pyridine (0.2 M), 4 h, 0 → 23 °C, 85%; c) NaN_3 (3.0 equiv), DMF (0.2 M), 12 h, 50 °C, 95%; d) 1.0 M NaOH/THF (1:2, 0.01 M), 12 h, 23 °C, 98%; e) ***4*** *(1.0 equiv),* ***5****, or* ***6*** *(1.2 equiv), NIS (2.2 equiv), MS (4 Å), TfOH (0.28 equiv), Et_2O/CH_2Cl_2 (4:1, 0.3 M), 2 h, −20 °C, 38–45%; f) TFA/CH_2Cl_2 (1:4, 0.02 M), 2 h, 0 → 23 °C, 99%; g) Me_3P (1 M in THF, 4.5 equiv), 0.1 M NaOH/THF (1:9), 4 h, 23 °C; h) $Pd(OH)_2$ (0.05 equiv), H_2, AcOH, 20 h, 23 °C, 65–70% (two steps); i)* ***9*** *(1.0 equiv),* ***6*** *(1.2 equiv), NIS (2.2 equiv), MS (4 Å), TfOH (0.28 equiv), Et_2O/CH_2Cl_2 (4:1, 0.04 M), 2 h, −20 °C, 50%; j) 1.0 M NaOH/THF (1:2, 0.02 M), 12 h, 23 °C, 94%; k) MsCl (1.2 equiv), pyridine (0.1 M), 4 h, 0 → 23 °C, 98%; l) NaN_3 (3.0 equiv), DMF (0.20 M), 12 h, 50 °C, 90%; m) TFA/CH_2Cl_2 (1:4, 0.02 M), 2 h, 0 → 23 °C, 99%; n) Me_3P (1 M in THF, 4.5 equiv), 0.1 M NaOH/THF (1:9), 4 h, 23 °C; o) $Pd(OH)_2$ (0.05 equiv), H_2, AcOH, 20 h, 23 °C, 85% (two steps); p) $LiBH_4$ (2 M in THF, 4.0 equiv), THF (0.07 M), 48 h, 70 °C, 77%; q) TBSCl (1.1 equiv), imidazole (2.0 equiv), DMF (0.11 M), 18 h, 0 → 23 °C, 38%; r) $(Boc)_2O$ (2.0 equiv), $Pd(OH)_2$, (0.05 equiv), H_2, EtOH (0.14 M), 18 h, 23 °C; s) TBSCl (1.1 equiv), imidazole (2.0 equiv), DMF (0.10 M), 18 h, 0 → 23 °C, 38% (two steps); t) MsCl (1.25 equiv), pyridine (0.22 M), 18 h, 0 → 23 °C, 99%; u) NaN_3 (2.0 equiv), DMF (0.17 M), 12h, 80 °C, 49%; v) TBAF (1.3 equiv), THF (0.06 M), 3 h, 23 °C, 99%; w)* ***14*** *(1.0 equiv),* ***5*** *(1.2 equiv), NIS (2.2 equiv), MS (4 Å), TfOH (0.28 equiv), Et_2O/CH_2Cl_2 (4:1, 0.3 M), 1 h, −20 °C, 30%; x) TFA/CH_2Cl_2 (1:4, 0.02 M), 2 h, 0 → 23 °C, 95%; y) Me_3P (1 M in THF, 4.5 equiv), 0.1 M NaOH/THF (1:9), 4 h, 23 °C; z) $Pd(OH)_2$ (0.05 equiv), H_2, AcOH, 20 h, 23 °C, 67% (two steps). Boc,* tert-*butoxycarbonyl; Ms, methanesulfonyl; DMF,* N,N-*dimethylformamide, NIS,* N-*iodosuccinimide; MS, molecular sieves; Tf, trifluoromethanesulfonyl; TFA, trifluoroacetic acid; TBS,* tert-*butyldimethylsilyl; TBAF, tetra-*n-*butylammonium fluoride; THF, tetrahydrofuran; Ac, acetyl; Cbz, benzyloxycarbonyl.*

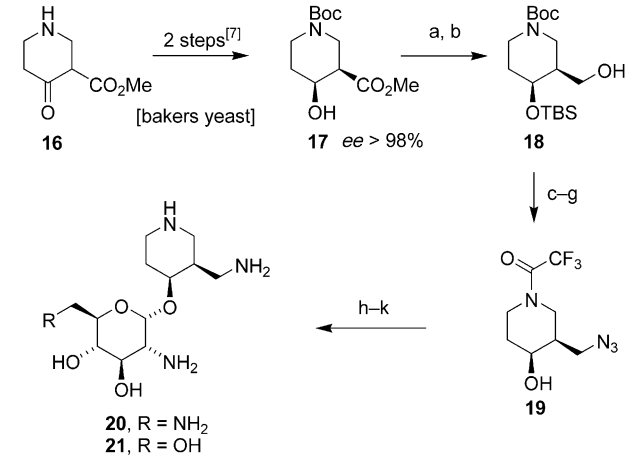

Scheme 2. Reagents and conditions: a) TBSCl (1.0 equiv), imidazole (2.0 equiv), DMAP (1.0 equiv), DMF (0.09 M), 0 → 23 °C, 24 h, 66%; b) $LiBH_4$ (2.0 M in THF, 2.0 equiv), 70 °C, 18 h, 82%; c) MsCl (1.25 equiv), pyridine (0.21 M), 0 → 23 °C, 18 h, 99%; d) NaN_3 (2.0 equiv), DMF (0.16 M), 80 °C, 16 h, 98%; e) TFA/CH_2Cl_2 (1:4, 0.02 M), 23 °C, 1.5 h, 98%; f) TFAA (1.5 equiv), Et_3N (1.5 equiv), CH_2Cl_2 (0.1 M), 23 °C, 1 h, 79%; g) TBAF (1.0 M in THF, 1.2 equiv), THF (0.06 M), 23 °C, 2 h, 85%; h) ***19*** *(1.0 equiv),* ***5****, or* ***6*** *(1.2 equiv), NIS (2.0 equiv), MS (4 Å), TfOH (0.2 equiv), Et_2O/CH_2Cl_2 (4:1, 0.04 M), 1 h, −20 °C, 25–30%; i) K_2CO_3 (5.0 equiv), $MeOH/H_2O$ (7:1, 0.03 M), 23 °C, 20 h, 64%; j) Me_3P (1.0 M in THF, 4 equiv), 0.1 M NaOH/THF (1:9), 4 h, 23 °C; k) $Pd(OH)_2$ (0.05 equiv), H_2, $AcOH/H_2O$ (1:1), 20 h, 23 °C, quantitative (two steps). TFAA, trifluoroacetic anhydride; DMAP, 4-dimethylaminopyridine.*

cleavage during a later synthetic step, the Boc group was replaced by Cbz. Simultaneous protection of the two hydroxy groups as the PMB acetal was achieved by treatment with *p*-methoxybenzaldehyde dimethyl acetal and TsOH. Subsequent reduction with $LiBH_4$ produced the intermediate **25**. The alcohol was converted into the azide in two steps, as described above. Finally, cleavage of the acetal with aq AcOH furnished the diol **26**. Glycosylation with **5** resulted in a mixture of three compounds. The two major products were isolated by chromatography, along with a smaller amount of the diglycosylated analogue. The two major components were subjected to the three-step deprotection protocol described above to afford the piperidine glycosides **1** and **27**. NMR spectroscopy identified the products as monoglycosylated compounds but did not provide sufficient information to assign their regioisomeric identities.

To resolve the ambiguity, a regioselective synthetic route was pursued (Scheme 3, steps l–r). The primary hydroxy group in **26** was selectively protected with TBSOTf and 2,6-lutidine, the remaining secondary alcohol was benzylated, and subsequent silyl deprotection with TBAF produced **28**. Glycosylation proceeded smoothly under standard conditions to afford, after deprotection, a piperidine glycoside that produced NMR spectra identical to those of **27**. Thus, the regioselective route provided unambiguous assignment of piperidine glycoside analogues **1** and **27**.

 © 2003 Wiley-VCH Verlag GmbH & Co. KGaA, Weinheim

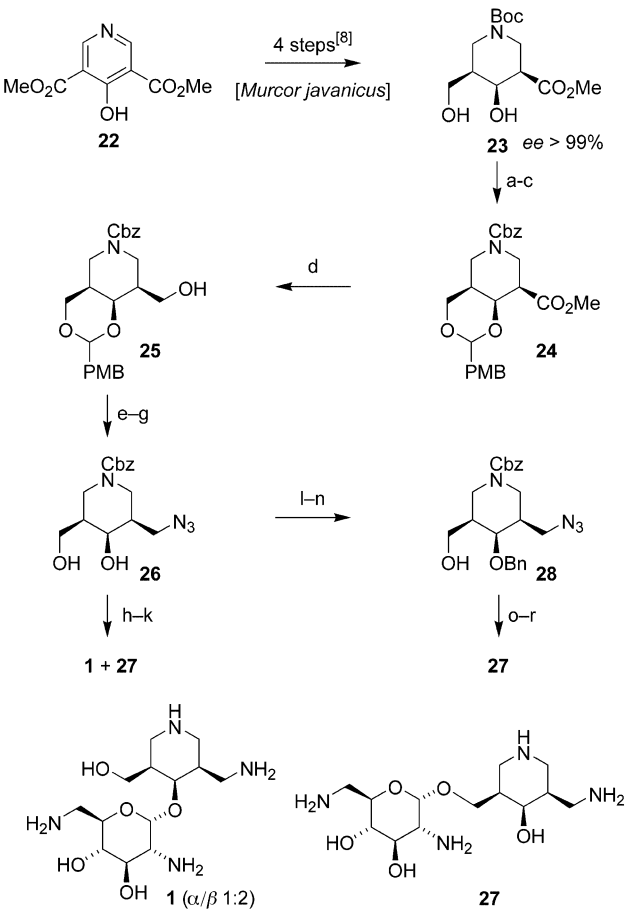

Scheme 3. *Reagents and conditions: a) TFA/CH_2Cl_2 (1:4, 0.16 M), 2 h, 0 → 23 °C, 98%; b) CbzCl (1.1 equiv), $NaHCO_3$ (5.0 equiv), H_2O/THF (1:1, 0.13 M), 12 h, 0 → 23 °C, 95%; c)* p*-methoxybenzaldehyde dimethyl acetal (1.5 equiv),* p*-TsOH (0.05 equiv), DMF (0.10 M), 5 h, 50 °C, 92%; d) $LiBH_4$ (2 M in THF, 3.0 equiv), THF (0.10 M), 3 h, 70 °C, 55%; e) MsCl (1.5 equiv), pyridine (0.10 M), 4 h, 0 → 23 °C, 98%; f) NaN_3 (3.0 equiv), DMF (0.10 M), 12 h, 50 °C, 96%; g) AcOH/H_2O (3:1, 0.05M), 3 h, 23 °C, 78%; h)* ***26*** *(1.0 equiv),* ***5*** *(1.2 equiv), NIS (2.2 equiv), MS (4 Å), TfOH (0.28 equiv), Et_2O/CH_2Cl_2 (4:1, 0.03M), 3 h, −20 → 0 °C, 25–28%; i) 8 M KOH/MeOH (1:1, 0.02 M), 1 h, 100 °C; j) Me_3P (1 M in THF, 4.5 equiv), 0.1 M NaOH/THF (1:9), 4 h, 23 °C; k) $Pd(OH)_2$ (0.05 equiv), H_2, AcOH, 20 h, 23 °C, 90% for* ***27*** *(two steps) and 86% for* ***1*** *(two steps); l) TBSOTf (1.3 equiv), 2,6-lutidine (2.0 equiv), CH_2Cl_2 (0.10 M), 2 h, 0 °C, 68%; m) NaH (2.0 equiv), BnBr (1.5 equiv), DMF (0.10 M), 2 h, 0 → 23 °C, 84%; n) TBAF (1.0 M in THF, 2.0 equiv), THF (0.05 M), 3 h, 0 → 23 °C, 81%; o)* ***28*** *(1.0 equiv),* ***5*** *(1.2 equiv), NIS (2.2 equiv), MS (4 Å), TfOH (0.28 equiv), Et_2O/CH_2Cl_2 (4:1, 0.01 M), 2 h, −20 °C, 45%; p) 8 M KOH/MeOH (1:1, 0.01 M), 3 h, 100 °C; q) Me_3P (1 M in THF, 4.5 equiv), 0.1 M NaOH/THF (1:9), 4 h, 23 °C; r) $Pd(OH)_2$ (0.05 equiv), H_2, AcOH, 20 h, 23 °C, 62% (three steps). PMB, 4-methoxybenzyl; Ts, toluenesulfonyl; Bn, benzyl.*

The biological activity of the novel piperidine glycosides as inhibitors of bacterial and eukaryotic protein synthesis, their binding affinity to the bacterial decoding-site target, and their potency against bacterial growth were evaluated by methods described in the preceding report[1] (Table 1). Among the piperidine compounds that were glycosylated at the 5-hydroxymethyl group (**7**, **8**, **11**, **15**, **27**), only the 6′-aminoglucosamine derivatives **7** and **27** of the *syn*-substituted piperidine scaffold inhibited bacterial in vitro translation (Table 1). In contrast to the active *syn*-piperidine derivative **7**, the *anti*-diastereomer **15** did not inhibit the translation assay, which illustrates the importance of the *syn*-relative stereochemistry. The presence of an additional hydroxy group in **27** resulted in a more than threefold increase in potency compared to **7** (IC_{50} = 74 and 260 μM, respectively). Replacement of the 6′-amino group at the glucosamine moiety in **7** by a hydroxy substituent led to a complete loss of activity for the derivative **8**, similar to the decrease in potency observed for the corresponding 2-DOS compounds neamine and paromamine (IC_{50} = 0.37 and 3.9 μM, respectively).[1]

Modification of the substitution pattern in the initially designed derivative **1** led to increased inhibition potency in the bacterial translation assay compared to the 4-hydroxy-modified compound **26** (IC_{50} = 35 and 74 μM, respectively). The potencies of **1** and **27** as inhibitors of bacterial translation were in line with their relative affinities for binding to the decoding-site RNA target (IC_{50} = 90 and 110 μM, respectively). Unlike the other piperidine derivatives, which were obtained as pure α-glycosides, compound **1** was isolated and tested as an inseparable 1:2 mixture of α- and β-anomers, which raises the question of what the biological activities of the individual components are. Molecular modeling studies suggested that both the α-anomer (Figure 1 c, d, e) and the β-anomer (Figure 2)

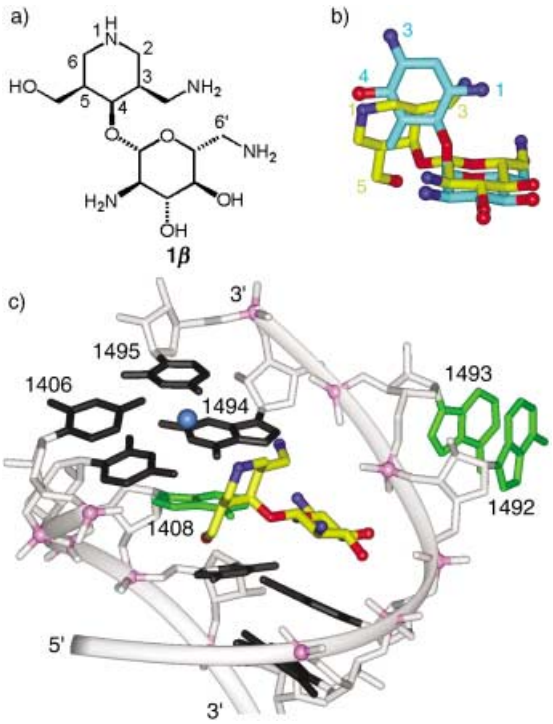

Figure 2. *a) The β-anomer of the designed piperidine glycoside* ***1****. b) Three-dimensional model of the β-anomer of* ***1*** *(yellow) superimposed on paromamine (blue) to show their conformational similarity. For clarity, the superimposed molecules have been slightly shifted apart along the y-axis. c) Model of the β-anomer of* ***1*** *(yellow) docked in the three-dimensional structure[2] of the bacterial decoding-site RNA. RNA bases are in dark grey and the sugar–phosphate backbone in light grey with phosphate groups emphasized in magenta. A water molecule participating in the non-Watson–Crick U1406◦U1495 base pair[3] and interacting with a 2-DOS hydroxy group is shown as a blue sphere. The flipped-out adenine residues 1492 and 1493, and the unpaired adenine 1408 are shown in green. The piperidine scaffold of* ***1*** *is participating in hydrogen-bond interactions with the carbonyl oxygen and N7 atoms of G1494, and with the amino group of A1408.*

 © 2003 Wiley-VCH Verlag GmbH & Co. KGaA, Weinheim

of **1** can be docked into the decoding-site RNA while forming favorable hydrogen-bond interactions. The related piperidine glycoside **20**, which was obtained as the α-anomer, did not inhibit the bacterial translation assay. The difference between **1** and **20** may be related to additional hydrogen-bond interactions of the 5-hydroxymethyl substituent with the RNA target. Since **1** was tested as a 1:2 mixture of α- and β-anomers, however, a direct comparison of potencies between **1** and **20** is inconclusive. The piperidine glycoside **21** did not show inhibition of bacterial translation, as was expected from the inactivity of **20** since 6′-hydroxy-substituted derivatives were generally less active than 6′-amino compounds (paromamine versus neamine,[1] and **8** versus **7**, see above).

The structure–activity relationships found for the synthetic piperidine glycosides show that the 3-(aminomethyl)piperidine scaffold does not confer a high potency comparable to that of the natural aminoglycosides. However, the piperidine derivatives yielded more potent inhibitors of bacterial translation than aminoglycoside mimetics containing acyclic scaffolds as replacements of 2-DOS, which are outlined in an accompanying report.[1] In contrast to the acyclic aminoglycoside mimetics, some of which displayed promiscuous inhibition of eukaryotic translation, the active piperidine glycosides were exclusively inhibitors of the bacterial system (Table 1). The conformationally restricted flexibility of the 3-(aminomethyl)piperidine scaffold might be responsible for both the higher activity and specificity of the piperidine glycosides towards the bacterial target.

Experimental Section

Characteristic analytical data of a representative piperidine glycoside (27): ^{1}H NMR (400 MHz, D_2O): $\delta = 5.17$ (d, $J = 3.6$ Hz, 1 H), 4.21 (brs, 1 H), 3.86 (brt, $J = 9.2$ Hz, 1 H), 3.82 (m, 1 H), 3.69 (brt, $J = 7.6$ Hz, 1 H), 3.58 (brt, $J = 8.0$ Hz, 1 H), 3.45–3.25 (m, 5 H), 3.17 (brd, $J = 7.6$ Hz, 1 H), 3.13 (brd, $J = 8.0$ Hz, 1 H), 3.05–2.95 (m, 3 H), 2.40–2.25 (m, 2 H) ppm; ^{13}C NMR (100 MHz, D_2O): $\delta = 95.5$, 71.2, 69.6, 68.5, 66.7, 62.9, 53.8, 40.6, 40.4, 40.3, 39.3, 38.4, 36.5 ppm; MS (ESI): *m/z* calcd for $C_{13}H_{29}N_4O_5$ $[M+H]^+$: 321.21; found: 321.2 (100 %).

We thank B. Aust for determining MIC values and Dr. K. Steffy for help with the eukaryotic in vitro translation assay. This work was supported in part by a National Institutes of Health grant to T.H.

[1] See the preceding communication: D. Vourloumis, G. C. Winters, M. Takahashi, K. B. Simonsen, B. K. Ayida, S. Shandrick, Q. Zhao, T. Hermann, *ChemBioChem* **2003**, *4*, 879–885.

[2] a) A. P. Carter, W. M. Clemons, D. E. Brodersen, R. J. Morgan-Warren, B. T. Wimberly, V. Ramakrishnan, *Nature* **2000**, *407*, 340–348; b) J. M. Ogle, D. E. Brodersen, W. M. Clemons, M. J. Tarry, A. P. Carter, V. Ramakrishnan, *Science* **2001**, *292*, 897–902.

[3] a) Q. Vicens, E. Westhof, *Structure* **2001**, *9*, 647–658; b) Q. Vicens, E. Westhof, *Chem. Biol.* **2002**, *9*, 747–755.

[4] Molecular modeling was performed by using published atom coordinates of the 30S ribosomal subunit–aminoglycoside complexes[2,3] and high-resolution crystal structures of synthetic RNA constructs containing the bacterial decoding-site internal loop (Q. Zhao, T. Hermann, unpublished results). Preferred conformations of the novel aminoglycoside mimetics **1** and **2** were explored by molecular dynamics simulations and energy minimization by using the Insight/Discover software (Accelrys, San Diego) and following established protocols (T. Hermann, E. Westhof, *J. Mol. Biol.* **1998**, *276*, 903–912; T. Hermann, E. Westhof, *J. Med. Chem.* **1999**, *42*, 1250–1261).

[5] a) K. Faber, *Biotransformations in Oganic Cemistry*, Springer, Berlin, **1997**; b) C.-H. Wong, G. M. Whiteside, *Enzymes in Synthetic Organic Chemistry*, Pergamon, Oxford, **1994**.

[6] a) B. Danieli, G. Lesma, D. Passarella, A. Silvani, *J. Org. Chem.* **1998**, *63*, 3492–3496; b) B. Danieli, G. Lesma, D. Passarella, A. Silvani, N. Viviani, *Tetrahedron* **1999**, *55*, 11 871–11 878.

[7] D. W. Knight, N. Lewis, A. C. Share, D. Haigh, *J. Chem. Soc. Perkin Trans. 1* **1998**, 3673–3683.

[8] X. Liang, A. Lohse, M. Bols, *J. Org. Chem.* **2000**, *65*, 7432–7437.

[9] a) D. Vourloumis, M. Takahashi, G. C. Winters, K. B. Simonsen, B. K. Ayida, S. Barluenga, S. Qamar, S. Shandrick, Q. Zhao, T. Hermann, *Bioorg. Med. Chem. Lett.* **2002**, *12*, 3367–3372; b) K. B. Simonsen, B. K. Ayida, D. Vourloumis, M. Takahashi, G. C. Winters, S. Barluenga, S. Qamar, S. Shandrick, Q. Zhao, T. Hermann, *ChemBioChem* **2002**, *3*, 1223–1228.

[10] S. Shandrick, Q. Zhao, Q. Hau, T. Hermann, unpublished work.

Received: June 12, 2003 [Z689]

 © 2003 Wiley-VCH Verlag GmbH & Co. KGaA, Weinheim